JACS
JOURNAL OF THE AMERICAN CHEMICAL SOCIETY
Article
pubs.acs.org/JACS

Forming B–B Bonds by the Controlled Reduction of a Tetraaryldiborane(6)

Thomas Kaese, Alexander Hübner, Michael Bolte, Hans-Wolfram Lerner, and Matthias Wagner*

Institut für Anorganische und Analytische Chemie, Goethe-Universität Frankfurt, Max-von-Laue-Straße 7, D-60438 Frankfurt am Main, Germany

Supporting Information

ABSTRACT: Dimeric aryl(hydro)boranes can provide suitable platforms for the synthesis of boron-containing graphene flakes through reductive B–B coupling. Two-electron reduction of 1,2:1,2-bis(4,4′-di-*tert*-butyl-2,2′-biphenylylene)diborane(6) (**4**) with LiNaph/THF establishes a B–B σ bond but can be accompanied by substituent redistribution. In the singly rearranged product, Li_2[**6**], only one 1,2-phenyl shift has occurred. The doubly ring-contracted product, Li_2[**7**], consists of two 9*H*-9-borafluorenyl moieties that are linked via their boron atoms. When the amount of LiNaph/THF is increased to 4 equiv, Li_2[**6**] is subsequently observed as the dominant species. Addition of 11 equiv of LiNaph/THF results in over-reduction with hydride elimination to afford the doubly boron-doped dibenzo[*g*,*p*]chrysene Li_2[**1**]. In contrast, excess KC_8 reduces **4** to the corresponding dihydrodibenzo[*g*,*p*]chrysene, K_2[**5**], with a *trans*-HB–BH core. Hydride abstraction from K_2[**5**] with 1 equiv of **4** leads to K[**8**], in which the central B–B bond is bridged by a single hydrogen atom. K[**8**] is also obtained upon treatment of **4** with 1 equiv of KC_8. All products have been characterized by multinuclear NMR spectroscopy and X-ray crystallography.

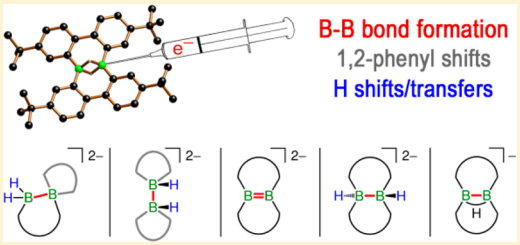

INTRODUCTION

Boron is among the most powerful electronically perturbative elements that can be incorporated into the core structures of fused polycyclic aromatic hydrocarbons (PAHs) in order to modify their optoelectronic properties.[1−13] Formally, a tricoordinate boron atom is isoelectronic to a carbenium ion. When the vacant p orbital efficiently interacts with the extended π-electron cloud of the surrounding all-carbon system, the absorption and emission maxima of the corresponding PAH shift to the red and charge mobilities are enhanced.[14] Applications of the resulting materials are very diverse and range from electron-transporting materials,[15] field-effect transistors,[13,16] supercapacitors,[17] and Li-ion batteries[18] to organic light-emitting devices[13] and solar cells.[19]

In the past, our group has prepared a number of 9,10-dihydro-9,10-diboraanthracene (DBA)[20−22] derivatives **A** (Figure 1), which turned out to be air and water tolerant, strongly fluorescent, and capable of accepting two electrons in a reversible manner.[7,8,23,24] Recently, the focus has been expanded toward the development of more extended core structures, such as **B** (Figure 1), which can be viewed not only as a stretched DBA but also as a doubly boron-bridged dibenzo[*g*,*p*]chrysene.[10,11] For a systematic assessment of key structure–property relationships, we next decided to move the two boron atoms from the outer rim of **B** to its central part. Even though the neutral molecule **C** (Figure 1) has so far remained elusive, we have already succeeded in the synthesis of its corresponding dianion, $[\mathbf{1}]^{2-}$ (Scheme 1).[25] While the dianion may find future applications in coordination chemistry,[26−28] neutral **C** would constitute a unique planar, ditopic Lewis acid with directly adjacent boron centers.

Li_2[**1**] is available via reduction of the C_1-symmetric 9*H*-9-borafluorene dimer **2**[29,30] with excess Li granules in THF (Scheme 1).[25] NMR spectroscopy shows that the dimeric framework of **2** gets quantitatively cleaved to the adduct **3** by THF at room temperature.[31] Electron injection apparently induces dimerization and skeletal rearrangements that annihilate the structural differences between the starting material **3** and the reaction product. Unfortunately, this process lacks the desired selectivity and therefore furnishes Li_2[**1**] in only moderate yields.

As a consequence, we will herein switch from **2**/**3** to compound **4**[29,30,32] (Scheme 1), which seems ideally preorganized for reductive B–B coupling.[33]

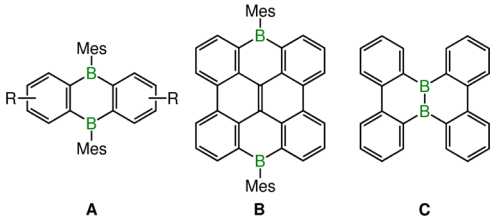

Figure 1. 9,10-Dihydro-9,10-diboraanthracenes (**A**), a doubly boron-bridged dibenzo[*g*,*p*]chrysene (**B**), and a related polycyclic aromatic hydrocarbon with central B–B core (**C**).

Received: March 2, 2016
Published: April 25, 2016

DOI: 10.1021/jacs.6b02303
J. Am. Chem. Soc. 2016, 138, 6224–6233

Scheme 1. Synthesis of $Li_2[1]$, Starting from 2 or 4

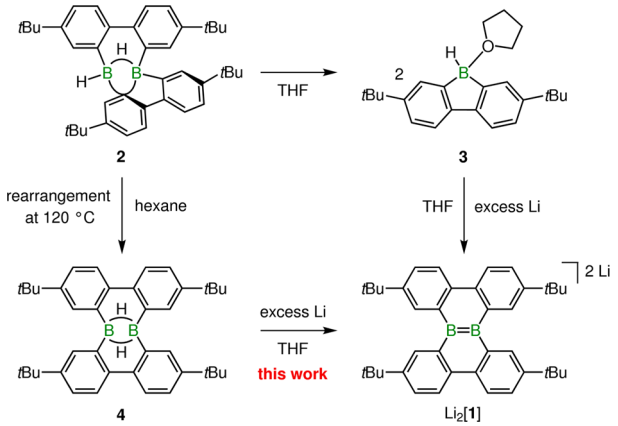

Apart from the role of **4** as a potential precursor of $Li_2[1]$, the reduction chemistry of its diboron core is fundamentally important in its own right. Interest dates back to the early days of A. Stock, who attempted to prepare $[H_3B{-}BH_3]^{2-}$ through reduction of B_2H_6.[34] The reaction was revisited several times[35] until 1994, when Shore et al. reported ^{11}B NMR evidence for the intermediate generation of $[H_3B{-}BH_3]^{2-}$, which reacts further to provide $[BH_4]^-$ and $[B_3H_8]^-$ as final products.[36] The first isolable molecules that came close to $[H_3B{-}BH_3]^{2-}$ were published in 2011/2014 by Matsuo and Tamao et al., who introduced exceptionally bulky phenyl groups (Ph*) to create isolable dianions $[(Ph^*)H_2B{-}BH_2(Ph^*)]^{2-}$ from diborane(6) precursors $H(Ph^*)B(\mu\text{-}H)_2B(Ph^*)H$.[37,38] Inspired by these results, our group recently managed to establish a B−B two-electron two-center (2e2c) bond within a BBC three-membered ring through reduction of a diborylmethane. The crystallographically characterized product represents the first example of a $[R_3B{-}BR_3]^{2-}$ anion.[39,40] By carefully adjusting the number of redox equivalents, even radicals containing B•B one-electron two-center (1e2c) bonds are accessible from ditopic triarylboranes and have been fully characterized.[39,41] Compared to the plethora of protocols developed for C−C bond formation, methods for selectively connecting two boron atoms are still scarce.[42] The simple addition of electrons to organoboranes may usefully expand the existing toolbox of reactions and therefore merits a detailed investigation.

In contrast to the vast majority of other B_2H_6 derivatives the two boron atoms of **4** are not just linked by hydrogen atoms, but also by two 2,2′-biphenylylene bridges. Given that partial rotation about the C−C single bonds is still possible, the molecular scaffold should retain sufficient conformational flexibility to support sp^2- as well as sp^3-hybridized boron atoms after reduction. The available structural options raise the following questions: *Is it possible to establish a B−B σ bond by trapping added electrons in the space amid the two boron atoms? Does over-reduction of diboranes(6) (such as **4**) with formal elimination of hydride substituents lead to B═B double-bonded species (such as $[1]^{2-}$)? What are the key factors governing the extent of substituent scrambling during reduction of diboranes(6)?* Answers are provided in this paper.

RESULTS AND DISCUSSION

Prior to the reduction of **4** by chemical means and on a preparative scale, its electrochemical properties were investigated by cyclic voltammetry and potentiostatic coulometry. In the cyclic voltammogram (Figure 2; room temperature; THF/$[nBu_4N][PF_6]$; vs FcH/FcH^+, FcH = ferrocene), **4** shows a single, irreversible reduction wave at E_{pc} = −2.74 V. Two irreversible oxidation events with peak potentials of E_{pa} = −2.17 and −1.97 V were recorded in the back scan. The irreversibility of the reduction process strongly indicates that a significant structural change is associated with the electron-transfer step.[43] Both boron atoms of **4** are tetracoordinate and therefore do not provide an energetically low-lying unoccupied orbital for the incoming electron (cf. the highly cathodic reduction potential of **4**).[44] Thus, electron injection should be accompanied at least by a hydrogen shift from the bridging to a terminal position.[37]

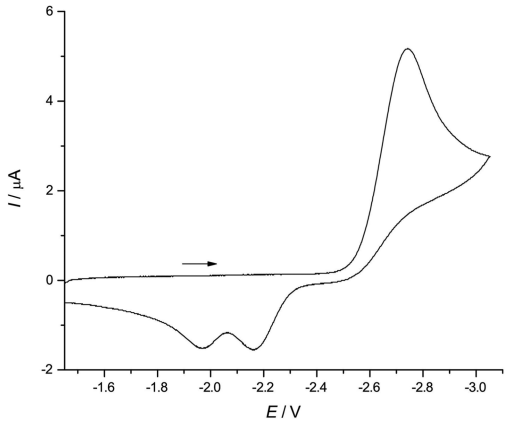

Figure 2. Cyclic voltammogram of **4** in THF at room temperature (vs FcH/FcH^+; supporting electrolyte, $[nBu_4N][PF_6]$ (0.1 mol L^{-1}); scan rate, 200 mV s^{-1}).

A coulometric measurement carried out at an applied potential of E_w = −3.0 V (THF; $[nBu_4N][PF_6]$) gave an electron count of approximately 1.5 e^- per molecule **4**. Coulometry on main-group compounds is notoriously problematic and tends to give a low electron count due to the inherent instability of radical species, reactions between the electrode products and still untransformed analyte molecules, or adsorption of the electrogenerated species to the electrode surface.[41,45] In the present case, the problem is aggravated by THF polymerization at the anode.[46] Given this background, our bulk electrolysis indicates that, in fact, two electrons could be delivered at the same potential value. For a two-electron reduction, the occurrence of only one irreversible reduction wave in the cyclic voltammogram again points toward a structural reorganization associated with one or both electron-transfer steps that leads to similar or inverted energetic potentials.[43] When dealing with the preparative reduction of **4**, one must therefore be aware of the possibility that doubly reduced **4** could already be generated while unconsumed starting material is still present.

In the following, the reduction of **4** by chemical means will be described. Since the outcome depends heavily on the reaction conditions applied, we will, for reasons of clarity, first restrict ourselves to an overview of the complex product distributions and discuss analytical details of the isolated products in a subsequent section. A third section is devoted to mechanistic considerations.

Product Distributions of the Reduction of 4 as a Function of the Reaction Conditions. Staying close to the published protocol,[25] we initially performed the alternative synthesis of $Li_2[1]$ from **4** at room temperature using excess Li in THF (Scheme 1). After workup, we isolated $Li_2[1]$, as its thf solvate $[Li(thf)_3]_2[1]$, in a 41% yield. $Li_2[1]$ also forms in

DOI: 10.1021/jacs.6b02303
J. Am. Chem. Soc. 2016, 138, 6224−6233

toluene, provided that a small volume of THF is added for Li^+ solvation (otherwise the reaction is negligibly slow). After filtration to remove unreacted Li, red single crystals of $[Li_2(thf)_3][\mathbf{1}]$, which contained 0.5 equiv of toluene molecules, precipitated from the cooled filtrate in a yield of 30% (see Figure 3, below).

Contrary to *a priori* expectations, even the highest yields of $Li_2[\mathbf{1}]$ gained from the reduction of **4** (41%) did not exceed the yields obtained from the reduction of **3** (43%). In order to identify relevant reaction intermediates and thereby to develop a deeper understanding of key mechanistic details, we investigated next the reduction of **4** under more controlled conditions. For this purpose, Li metal was replaced by LiNaph/THF (LiNaph = lithium naphthalenide). Use of the homogeneous reducing agent should accelerate electron-transfer rates, circumvent surface effects, and facilitate the precise adjustment of the number of added redox equivalents.

First, we targeted the lithium hydridoborate $Li_2[\mathbf{5}]$ (Scheme 2), which features an electron-precise B−B single bond and is a

Scheme 2. Major Products Formed upon Reduction of Compound 4 with 2 or 4 equiv of LiNaph/THF in Toluene at −78 °C[a]

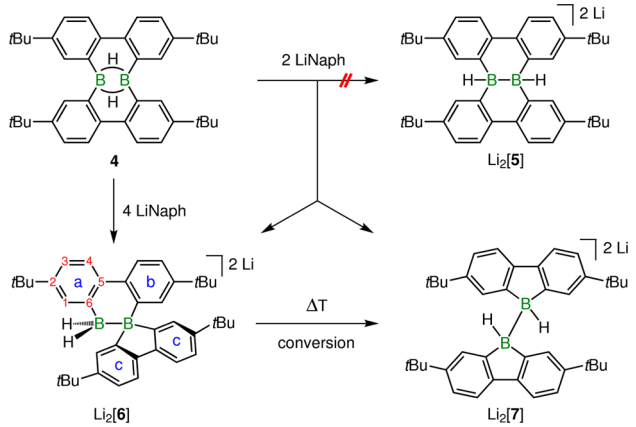

[a]At moderately elevated temperatures, $Li_2[\mathbf{6}]$ rearranges to $Li_2[\mathbf{7}]$.

conceivable intermediate on the way from **4** to $Li_2[\mathbf{1}]$. The requisite two-electron reduction of **4** was performed by adding 2 equiv of LiNaph/THF at −78 °C in toluene. The reaction did not furnish $Li_2[\mathbf{5}]$, but rather its rearranged isomers $Li_2[\mathbf{6}]$ and $Li_2[\mathbf{7}]$ (Scheme 2). The experiment was repeated several times. $Li_2[\mathbf{6}]$ and $Li_2[\mathbf{7}]$ always remained major products, but their relative ratios varied to a certain extent (^{1}H NMR spectroscopic control of the crude product). Notably, $Li_2[\mathbf{6}]$ tends to transform to $Li_2[\mathbf{7}]$, promoted by apolar solvents and elevated temperatures (Scheme 2; NMR spectroscopic monitoring during workup). From a representative experiment, $Li_2[\mathbf{7}]$ could be isolated in a yield of 51%. Single crystals of $[Li(thf)]_3[Li][\mathbf{7}]_2$ grew from pentane at room temperature (see Figure 5, below). Like $Li_2[\mathbf{5}]$, the compounds $Li_2[\mathbf{6}]$ and $Li_2[\mathbf{7}]$ are diborane(6) dianions. As planned, B−B 2e2c bonds have been established through reduction of the diborane(6) precursor. However, under the conditions applied, the desired transformation was accompanied by substituent scrambling, leading to ring-contraction reactions.

$Li_2[\mathbf{6}]$ formed preferentially over $Li_2[\mathbf{7}]$ when the amount of reducing agent was increased from 2 equiv to 4 equiv of LiNaph/THF (toluene, −78 °C). After workup, $Li_2[\mathbf{6}]$ was isolated in 23% yield by precipitation from THF at −30 °C. Single crystals of $[Li(thf)_3][Li(thf)_2][\mathbf{6}]$ were grown from more dilute THF solutions (see Figure 4, below). As a side product, we observed small quantities of $Li_2[\mathbf{1}]$, even though its putative precursor, $Li_2[\mathbf{5}]$, was still not detectable in the reaction mixture.

In the presence of 11 equiv of LiNaph/THF, **4** furnished only small amounts of $Li_2[\mathbf{6}]$, whereas $Li_2[\mathbf{1}]$ became the dominant product (THF-d_8; NMR spectroscopic control of the crude reaction mixture). The separation of $Li_2[\mathbf{1}]$ from unreacted LiNaph was successfully accomplished by fractional crystallization. As a drawback, however, quantitative removal of co-precipitated naphthalene through hexane extraction results in yield losses, because the solubility of $Li_2[\mathbf{1}]$ in hexane is significant.

Since it should be easier to separate organoboron products from insoluble graphite rather than from naphthalene, we next attempted the synthesis of $K_2[\mathbf{1}]$ from **4** using excess KC_8 (20 equiv, THF, room temperature). Yet, it turned out that the nature of the alkali metal (cation) has a decisive influence on the reaction outcome: instead of $K_2[\mathbf{1}]$, the initial target anion $[\mathbf{5}]^{2-}$ (Scheme 3) formed reproducibly in a highly selective transformation (83% isolated yield). $[K_2(thf)_4][\mathbf{5}]$ crystallized from THF in the form of deep orange blocks (see Figure 6, below).

Scheme 3. Reduction of 4 with 20 equiv or 1 equiv of KC_8 Proceeds without Rearrangement of the Original Backbone and Leads to $K_2[\mathbf{5}]$ or $K[\mathbf{8}]$, Respectively

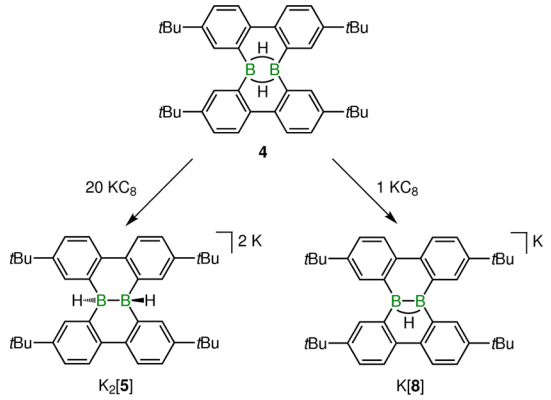

Interestingly, the reactivity differences between KC_8 and LiNaph become less pronounced when fewer reduction equivalents are employed (Table 1). For comparability reasons, these experiments were performed in toluene containing a small volume of added THF. According to ^{1}H and ^{11}B NMR spectroscopy, reaction of **4** with 4 equiv of KC_8 mainly yielded $K_2[\mathbf{6}]$ together with $K_2[\mathbf{5}]$; as a reminder, LiNaph gave $Li_2[\mathbf{6}]$ and small amounts of $Li_2[\mathbf{1}]$ under these conditions. Addition of 2 equiv of KC_8 to **4** afforded $K_2[\mathbf{6}]$, $K_2[\mathbf{7}]$, and approximately 10% of the singly hydrogen-bridged species $K[\mathbf{8}]$. The anions $[\mathbf{6}]^{2-}$ and $[\mathbf{7}]^{2-}$ are known from the corresponding LiNaph reduction, whereas $[\mathbf{8}]^-$ is a newly observed compound.

With the aim to access $K[\mathbf{8}]$ on a preparative scale, the stoichiometric ratio between **4** and KC_8 was systematically varied. It finally turned out that use of 1 equiv of KC_8 in THF provided $K[\mathbf{8}]$ in yields of 58% (Scheme 3). Yellow crystals of

DOI: 10.1021/jacs.6b02303
J. Am. Chem. Soc. 2016, 138, 6224−6233

Table 1. Major Products (≥30%, shown in bold) and Minor Products (≥10%) of the Reduction of 4 in Toluene or *THF* (shown in italics) According to NMR Spectroscopy (THF-d_8)

red. agent	equiv	products	red. agent	equiv	products
LiNaph	2	**Li_2[6]**, **Li_2[7]**	KC_8	2	**K_2[6]**, **K_2[7]**, K[8]
LiNaph	4	Li_2[1], **Li_2[6]**	KC_8	4	K_2[5], **K_2[6]**
LiNaph	11	***Li_2[1]***, *Li_2[6]*	KC_8	20	***K_2[5]***
Li	60	***Li_2[1]***, ***Li_2[6]***			
Li	125	**Li_2[1]**, **Li_2[6]**			

$[K(thf)_2][\mathbf{8}]$ were grown from THF/hexane (see Figure 7, below).

Finally, coming back again to the initial transformation of **4** with excess Li metal in THF, we were now able to identify the NMR signature of Li_2[**6**] in spectra recorded on the crude reaction mixtures. Both compounds, Li_2[**1**] and Li_2[**6**], reproducibly appeared in almost equimolar ratio, which answers our initial question regarding the 41% yield of Li_2[**1**]. Subsequent attempts to promote Li_2[**1**] formation by accelerating the hydride abstraction through added Me_3SiCl led to only marginally improved yields. The presence of the chlorosilane nevertheless had a beneficial effect, because it facilitated the workup process.[25] Instead of Li_2[**6**] (and some other side products), mainly lithium 9-trimethylsilyl-9-hydrido-boratafluorene[25] formed (together with Li_2[**1**]) and remained in solution under the conditions applied to crystallize the boron-doped PAH.

Characterization of the Reduction Products. *Solid-State Structure of $[Li_2(thf)_3]$[1].* Compound $[Li_2(thf)_3][\mathbf{1}]$ exists as a coordination polymer in the solid state. Within each polymer chain, dianions $[\mathbf{1}]^{2-}$ are linked by $[Li_2(thf)_3]^{2+}$ aggregates, in which two Li^+ cations share three thf ligands (Figure 3). The asymmetric unit of the crystal contains two

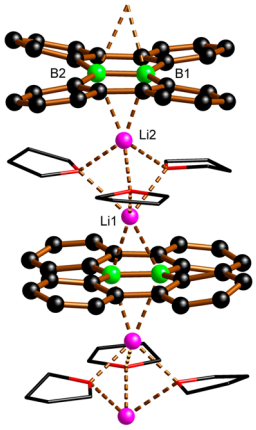

Figure 3. One strand of the coordination polymer $[Li_2(thf)_3][\mathbf{1}]$ in the solid state. *t*Bu groups and C*H* atoms are omitted for clarity.

crystallographically independent polymer subunits (I and II) with similar geometric parameters, leading to $\{I\}_\infty$ and $\{II\}_\infty$ strands. The B═B bond lengths amount to 1.641(6) Å (subunit I)/1.627(6) Å (subunit II), and all Li···B distances within the contact ion pairs fall in the narrow range between 2.413(9) Å and 2.525(9) Å. Compared to the solid-state structure of $[Li(thf)_3]_2[\mathbf{1}]$, which crystallizes as discrete inverse sandwich complexes,[25] the B═B bonds in polymeric $[Li_2(thf)_3][\mathbf{1}]$ are slightly elongated (Δ_{av} = 0.026 Å), while the Li···B contacts are contracted (Δ_{av} = −0.089 Å). Similar to the all-carbon relative dibenzo[*g*,*p*]chrysene,[47] steric repulsion between *ortho*-H atoms of adjacent phenylene rings forces the $[\mathbf{1}]^{2-}$ scaffolds out of planarity. The two 2,2′-biphenylylene bridges within the same $[\mathbf{1}]^{2-}$ anion possess opposite curvatures.

Solid-State Structure and NMR Data of Li_2[6]. The all-carbon congener of the dianion $[\mathbf{6}]^{2-}$ is already known and possesses a spirocyclic framework, composed of a 9,10-dihydrophenanthrene molecule that is fused with a fluorene moiety.[48] From this compound, $[\mathbf{6}]^{2-}$ can formally be generated through an exchange of the two aliphatic carbon atoms for tetracoordinate borate anions. In the solid state, the central B_2C_4 ring adopts the characteristic twisted 1,3-cyclohexadiene conformation with torsion angles C(21)−C(22)−C(32)−C(31) = −31.0(4)° and B(1)−B(2)−C(22)−C(32) = 44.6(2)°. The B(1)−B(2) bond length of $[\mathbf{6}]^{2-}$ amounts to 1.810(5) Å, and is therefore larger by 0.021 Å than the B−B bond length of $[\mathbf{7}]^{2-}$ (see below). For comparison, in the typical isoelectronic $C(sp^3)-C(sp^3)$ single bond, the two carbon atoms are only 1.54 Å apart.[49] The ligand sphere of B(1) in $[Li(thf)_3][Li(thf)_2][\mathbf{6}]$ deviates significantly from an ideal tetrahedral geometry, because the C(1)C(11)-C(31) basal plane is distorted due to the small angle C(1)−B(1)−C(11) = 98.2(3)° within the five-membered ring. Moreover, the B(2)−B(1) vector does not run perpendicular to the C_3 plane: the endocyclic angle C(31)−B(1)−B(2) = 99.6(3)° is significantly compressed, while the exocyclic angle C(11)−B(1)−B(2) = 119.8(3)° is expanded to a value normally observed for sp^2-hybridized boron centers. Contrary to B(1), B(2) features an essentially unstrained environment (B(1)−B(2)−C(21) = 104.3(3)°). $[Li(thf)_3][Li(thf)_2][\mathbf{6}]$ forms contact-ion pairs in the crystal lattice. The $[\mathbf{6}]^{2-}$ ion binds each of its Li^+ counterions in a chelating manner through one B*H* hydride substituent and one boron-bonded carbon atom. $Li(1)^+$, which carries only two thf ligands, establishes the shorter Li−C contact (2.327(7) Å), while $Li(2)^+$ (three thf ligands) binds at a longer Li−C distance (2.639(7) Å). The above-mentioned widening of the C(11)−B(1)−B(2) angle may be associated with $Li(1)^+$ chelation (Figure 4).

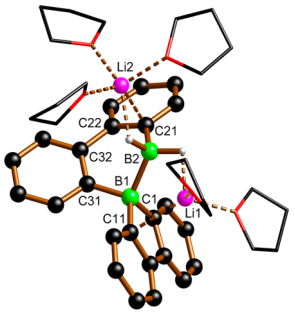

Figure 4. Molecular structure of $[Li(thf)_3][Li(thf)_2][\mathbf{6}]$ in the solid state. *t*Bu groups and C*H* atoms are omitted for clarity.

DOI: 10.1021/jacs.6b02303
J. Am. Chem. Soc. 2016, 138, 6224−6233

NMR spectra of Li_2[**6**] were recorded in THF-d_8. In the $^{11}B\{^1H\}$ NMR spectrum, the compound gives rise to two resonances at −11.0 ppm and −19.9 ppm (cf. Li_2[**7**]: −13.4 ppm). Upon proton coupling, the width at half height of the signal at −19.9 ppm doubles (R_2BH_2), whereas that of the other resonance remains unchanged (R_4B). Three sets of ^1H aryl resonances are detectable for Li_2[**6**]. Two of those are well-resolved at room temperature (H-a, H-b), while the third set consists of very broad signals, each of them integrating 2H (H-c; Scheme 2). At a measurement temperature of 50 °C and a spectrometer field strength of 250 MHz (instead of 500 MHz), the ill-defined proton signals become considerably sharpened. This indicates a dynamic behavior of the system in solution, which likely arises from conformational changes of the twisted B_2C_4 ring and/or from an association−dissociation equilibrium between the $[Li(thf)_n]^+$ and $[\mathbf{6}]^{2-}$ ions. According to a 2D $^1H,^{13}C$ HMBC experiment (500 MHz, room temperature), all six well-resolved proton resonances belong to the same biphenyl unit. Correspondingly, the poorly resolved signals arise from the second biphenyl fragment of $[\mathbf{6}]^{2-}$. The benzene rings marked "a" and "b" in Scheme 2, are necessarily different from each other. In contrast, both benzene rings "c" can become magnetically equivalent as soon as fast intramolecular motion leads to an average C_s symmetry of the molecular scaffold. We therefore assign the set of broad resonances to the 9-borafluorene fragment. The two remaining signal sets were assigned to the rings "a" and "b" by means of an $^1H,^{11}B$ correlation experiment, which showed a cross peak between one *ortho*-H signal and the BH_2 boron signal (a), while the second *ortho*-H atom was correlated with the other boron atom (b).

*Solid-State Structure and NMR Data of Li_2[**7**].* According to X-ray diffraction on a crystal of $[Li(thf)]_3[Li][\mathbf{7}]_2$, the dianion $[\mathbf{7}]^{2-}$ consists of two 9*H*-9-borafluorene molecules that are linked through an electron pair to form a B−B single bond (Figure 5).

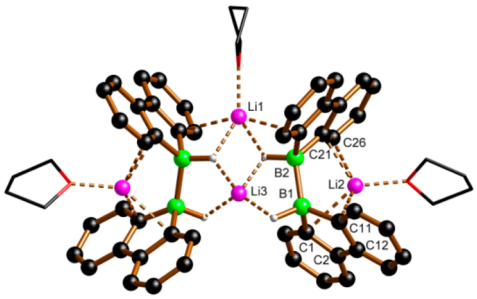

Figure 5. Molecular structure of $[Li(thf)]_3[Li][\mathbf{7}]_2$ in the solid state. *t*Bu groups and C*H* atoms are omitted for clarity.

The corresponding B(1)−B(2) bond length of 1.789(7) Å is slightly shorter than that of a related electron-precise diborate (1.83(2) Å), which Power et al. obtained through the reduction of 2,6-$Trip_2C_6H_3BBr_2$ with KC_8 (Trip = 2,4,6-triisopropylphenyl).[50] We also emphasize that the all-carbon analogue of $[\mathbf{7}]^{2-}$, i.e., 9,9′-bifluorenyl, has been synthesized through reductive coupling of 9-bromofluorene with a variety of reducing agents.[51] In the crystal lattice of $[Li(thf)]_3[Li][\mathbf{7}]_2$, two dianions are linked by $Li(1)^+$ and $Li(3)^+$ to give a C_2-symmetric dimer. The $Li(3)^+$ ion is surrounded by four B*H* hydride substituents in a strongly distorted tetrahedral fashion; both $[\mathbf{7}]^{2-}$ ions act as chelating ligands. $Li(1)^+$ possesses a coordination number of five with close contacts to two B*H* hydride substituents and two boron-bonded carbon atoms. The coordination sphere is completed by one thf molecule. Reminiscent of an *ansa*-metallocene structure, the $[Li(2)(thf)]^+$ ion occupies the pocket built by the two 9-borafluorenyl units of $[\mathbf{7}]^{2-}$.[52]

The ^{11}B NMR resonance of Li_2[**7**] in THF-d_8 appears as a doublet at −13.4 ppm with a $^1J(B,H)$ coupling constant of 71 Hz. Both values are in good agreement with those reported for Power's compound.[50] The signal of the B*H* hydrogen atom is broadened almost beyond detection in the ^1H NMR spectrum. Its chemical shift value of 2.1 ppm was finally determined with the help of a $^1H,^{11}B$-HSQC experiment. NMR spectroscopy further shows the four aryl rings of Li_2[**7**] to be magnetically equivalent at room temperature, thereby indicating free librational motion about the B−B axis on the NMR time scale.

*Solid-State Structure and NMR Data of K_2[**5**].* Similar to $[Li_2(thf)_3][\mathbf{1}]$, $[K_2(thf)_4][\mathbf{5}]$ forms coordination polymers in the crystal lattice, which consist of twisted $[\mathbf{5}]^{2-}$ dianions linked by $[K_2(thf)_4]^{2+}$ aggregates (Figure 6).

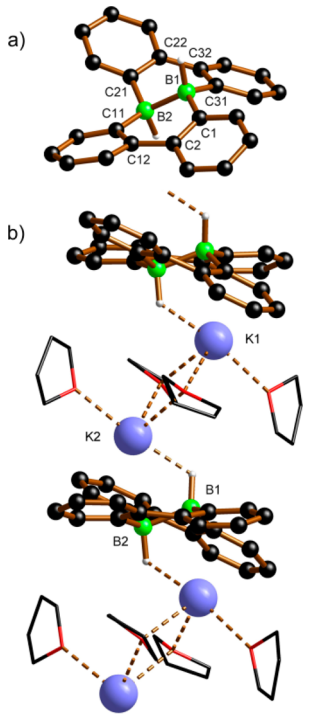

Figure 6. Molecular structures of the anion $[\mathbf{5}]^{2-}$ (a) and its coordination polymer $[K_2(thf)_4][\mathbf{5}]$ (b) in the solid state. *t*Bu groups and C*H* atoms are omitted for clarity.

The central B(1)−B(2) bond (1.755(4) Å) is longer by Δ_{av} = 0.12 Å than the B═B double bonds in $[Li_2(thf)_3][\mathbf{1}]$ (two crystallographically independent polymer strands) and therefore falls in the range of B−B single bonds. We have previously published the calculated molecular structure of the hypothetical neutral compound **5′**,[29] that corresponds to a molecule of **4** in which the bridging hydrogen atoms have been shifted into terminal positions to create electron deficient, three-coordinate boron centers. The B···B distance in **5′** amounts to 2.591 Å. Thus, the injection of two electrons into the molecule pulls the two boron atoms closer together by 0.836 Å (cf. ref 39 for a closely related experimentally assessed redox pair). Also for $[\mathbf{5}]^{2-}$, an all-carbon equivalent exists, i.e., 8b,16b-dihydro-

DOI: 10.1021/jacs.6b02303
J. Am. Chem. Soc. 2016, 138, 6224−6233

dibenzo[*g*,*p*]chrysene.[48,53] Thus, both the H−B−B−H and the H−C−C−H cores are compatible with the geometric constraints imposed by two 2,2′-biphenylylene bridges. While *cis* and *trans* configurations are known for 8b,16b-dihydrodibenzo[*g*,*p*]chrysene,[53] the crystal structure analysis of $[K_2(thf)_4][\mathbf{5}]$ revealed exclusively the *trans* isomer with a corresponding torsion angle H(1)−B(1)−B(2)−H(2) of −159(2)°. In fact, the entire transformation of **4** to $K_2[\mathbf{5}]$ appears to be *trans* selective, because the crude product $K_2[\mathbf{5}]$ also gave rise to only one set of signals in the ^{1}H and ^{13}C NMR spectra.

In the ^{11}B NMR spectrum of $K_2[\mathbf{5}]$, ^1J(B,H) coupling is not resolved, but the ^{11}B chemical shift value (−17.9 ppm) is highly diagnostic: it nicely agrees with the shift value of isomer $Li_2[\mathbf{7}]$ (−13.4 ppm), but differs greatly from that of the dehydrogenated congener $Li_2[\mathbf{1}]$ (32 ppm[25]). The boron-bonded hydrogen atoms give rise to one broad ^{1}H NMR signal at 1.7 ppm. All four benzene rings are magnetically equivalent at room temperature in solution.

*Solid-State Structure and NMR Data of K[**8**].* The asymmetric unit of $[K(thf)_2][\mathbf{8}]$ contains a twisted monoanionic molecular flake featuring a single μ-H atom that bridges a short B(1)−B(2) bond of 1.651(6) Å (Figure 7a).

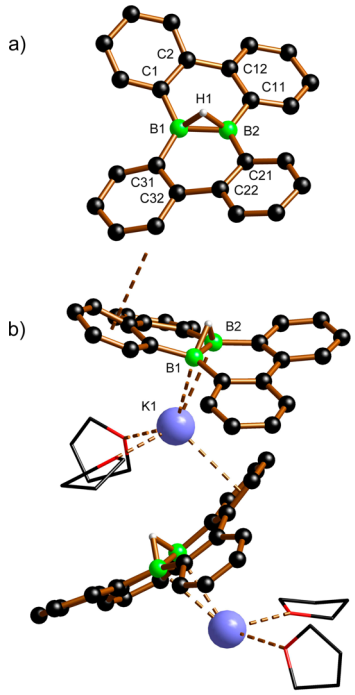

Figure 7. Molecular structures of the anion $[\mathbf{8}]^-$ (a) and its coordination polymer $[K(thf)_2][\mathbf{8}]$ (b) in the solid state. *t*Bu groups and C*H* atoms are omitted for clarity.

This value is close to the average B═B bond length in $[Li_2(thf)_3][\mathbf{1}]$ (1.634 Å), but smaller by 0.10 Å than the B−B bond length in $[K_2(thf)_4][\mathbf{5}]$ (1.755(4) Å). The C−B−C/B bond angles about B(1) as well as B(2) in $[\mathbf{8}]^-$ sum up to 360°, again similar to the structure of $[\mathbf{1}]^{2-}$ but in stark contrast to that of $[\mathbf{5}]^{2-}$ ($\sum$(C−B−C/B) = 335°, 338°). These results are in line with theoretical works on $[(\mu\text{-H})H_2BBH_2]^-$. For this anion, Lammertsma et al. calculated a distance between both boron atoms of 1.624 Å and concluded that the central part of the molecule can be thought to result from protonation of a B═B bond.[54] Moreover, for the related system [(μ-H)(Eind)-HBBH(Eind)]$^-$, Tamao et al. observed a B···B distance of 1.655(2) Å and claimed that this indicated double-bond character of the diboron core (Eind = 1,1,3,3,5,5,7,7-octaethyl-*s*-hydrindacen-4-yl).[37] The K^+ counterion coordinates both B atoms from the side opposite to the μ-H atom. The coordination sphere is completed by two thf ligands and the aryl ring of an adjacent $[\mathbf{8}]^-$ anion to form a coordination polymer (Figure 7b).

The ^{11}B NMR spectrum of K[**8**] further confirms a certain degree of B═B double-bond character within the diboron core. The broad ^{11}B signal (20.4 ppm) lies relatively near to that of $Li_2[\mathbf{1}]$ (32 ppm),[25] but is downfield-shifted by 38.3 ppm compared to the resonance of $K_2[\mathbf{5}]$ (−17.9 ppm). According to the ^{1}H and ^{13}C NMR spectra, all aryl rings contained in K[**8**] are magnetically equivalent at room temperature in solution. A broadened proton signal was detectable at −0.99 ppm, which sharpened upon ^{11}B decoupling; its integral value equals a quarter of the integral value of each aryl proton resonance. The signal is therefore assignable to the boron-bonded hydrogen atom.

Mechanistic Considerations. Up to this point, we have unveiled the behavior of **4** under reducing conditions in dependence of the number of redox equivalents employed and the reducing agents chosen. Some of the transformations are highly selective (cf. the synthesis of $K_2[\mathbf{5}]$), others lead to product mixtures containing two or three dominant species (Table 1). In all cases, the major products have been isolated and characterized by NMR spectroscopy and X-ray crystallography. On the basis of the data obtained, we can now identify common motifs between the individual reactions and finally propose a mechanistic model to explain the complex scenario.

*Hydride Transfer and Hydride Elimination Processes in the Course of the Reduction of **4**.* First, we consider the reduction of **4** with a large excess of reducing agent. Use of LiNaph/THF leads to $Li_2[\mathbf{1}]$, whereas KC_8 gives $K_2[\mathbf{5}]$. The $[\mathbf{1}]^{2-}$ anion can conceivably be generated from $[\mathbf{5}]^{2-}$ if (i) a hydride scavenger is present to create three-coordinate boron intermediates and (ii) the number of redox equivalents supplied suffices to alleviate the resulting electron deficiency at boron by establishing a B═B double bond. The small, hard Li^+ ion constitutes a stronger Lewis acid than the larger K^+ ion, and the heat of formation of LiH (−91 kJ mol^{-1}) exceeds that of KH (−56 kJ mol^{-1}) by 35 kJ mol^{-1}.[55] Consequently, Li^+ could well take the role of a hydride scavenger while K^+ is much less likely to do so. Hydride elimination is not an issue when **4** is treated with only 2 equiv of LiNaph/THF or KC_8, because the number of electrons available is too small to compensate for the loss of a hydride substituent. Therefore, the same anions are generated ($[\mathbf{6}]^{2-}$, $[\mathbf{7}]^{2-}$), irrespective of the selected reducing agent. Upon addition of 4 reduction equivalents to **4**, we are facing an intermediate situation where mostly $[\mathbf{6}]^{2-}$ is accompanied by $Li_2[\mathbf{1}]$ (LiNaph/THF) or $K_2[\mathbf{5}]$ (KC_8).

The argumentation outlined above does not account for the synthesis of K[**8**] (about 50%) from **4** and 1 equiv of KC_8. The anion $[\mathbf{8}]^-$ contains one hydrogen substituent less than **4** or $[\mathbf{5}]^{2-}$, even though the potential hydride scavenger Li^+ is missing. As an alternative pathway, $[\mathbf{8}]^-$ formation might be triggered by an interaction between already reduced product molecules, $K_2[\mathbf{5}]$, and not yet consumed **4** (note the electrochemical investigations outlined above, which support such a scenario). Compound **4** still is a potential Lewis acid and could therefore engage in hydride-exchange reactions. This possibility is particularly relevant when electrons are in short

DOI: 10.1021/jacs.6b02303
J. Am. Chem. Soc. 2016, 138, 6224−6233

supply (as in the present case), because otherwise the concentration of neutral **4** will rapidly decrease such that it becomes less available for hydride abstraction.

To scrutinize this hypothesis, we prepared a 1:1 mixture of K_2[**5**] and **4** in THF-d_8 and monitored it by NMR spectroscopy after the orange color of K_2[**5**] had faded (Scheme 4). The

Scheme 4. Three Major Compounds Are Generated from 4 and K_2[5]; K[9] and K_2[10] Are Also the Products of the Reaction Between 4 and KH[a]

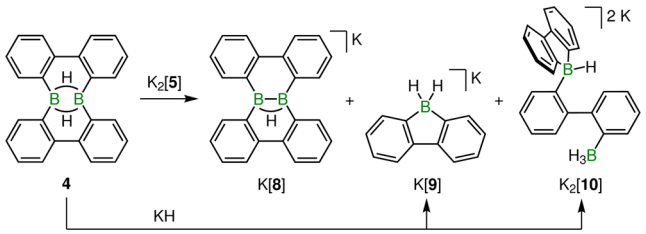

[a]Room temperature, THF; *t*Bu groups are omitted for clarity).

NMR signals of **4** and K_2[**5**] had completely vanished and the resonances of K[**8**] had appeared instead. However, the NMR spectra gave no indication for a hydride adduct [**4**·H]$^-$, which should adopt the highly symmetric bridged structure [Ar_2(H)-B(μ-H)B(H)Ar_2]$^-$.[56]

A plausible explanation would be that [**4**·H]$^-$ possesses only a short lifetime and rapidly rearranges to other products. As a test, we charged an NMR tube with a mixture of **4** and excess KH in THF-d_8 (Scheme 4). The reaction was rather slow, likely due to the limited solubility of KH in THF. Nevertheless, **4** was consumed after 2 weeks and the resonances assignable to K[**9**] (cf. ref 25) were prominent in the ^{1}H and ^{11}B NMR spectra. Moreover, crystals of [K(thf)$_3$][K(thf)][**10**] precipitated in the NMR tube (Figure 8; cf. the SI for a structure discussion). Despite its poor solubility, the ^{1}H and ^{11}B NMR signals of K_2[**10**] could be determined in THF-d_8. Afterward, we

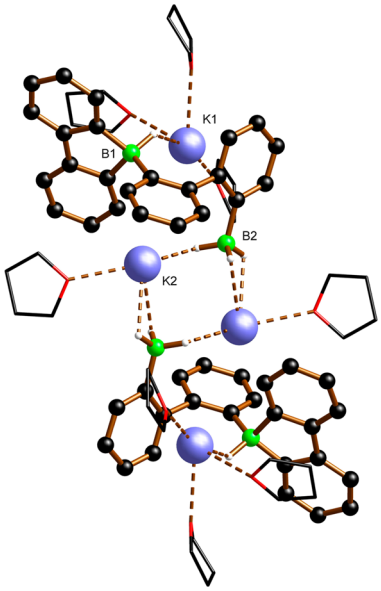

Figure 8. Molecular structure of [K(thf)$_3$][K(thf)][**10**] in the solid state. *t*Bu groups and C*H* atoms are omitted for clarity.

identified the resonance patterns of K[**9**] and K_2[**10**] also in the NMR spectra of the **4**/K_2[**5**] mixture (Scheme 4).

In conclusion, the products obtained from the reaction of **4** and K_2[**5**] support the assumption that K[**8**] can be generated through hydride transfer from K_2[**5**] to **4**. The resulting hydride adduct [**4**·H]$^-$ would subsequently turn into K[**9**] and K_2[**10**]. Remarkably, the ^{1}H NMR spectrum recorded on the **4**/K_2[**5**] sample was almost identical to the spectrum of the crude product mixture gained from **4** and 1 equiv of KC_8 (cf. the SI for plots of the spectra). In line with our initial suggestion, this points toward a similar hydride transfer process also in this case, after the KC_8 has converted half of **4** into K_2[**5**].

Skeletal Rearrangement Processes in the Course of the Reduction of **4**. The reduction of **4** can be carried out in a way to preserve the original molecular backbone (cf. Li_2[**1**], K_2[**5**], K[**8**]). Yet, under certain conditions 1,2-phenyl shifts occur, resulting in ring contraction and furnishing Li_2[**6**]/Li_2[**7**]. Related phenyl shifts are known for comparable PAHs: A classical synthesis of dibenzo[*g*,*p*]chrysene ($\triangleq$ Li_2[**1**]) takes advantage of the Clemmensen reduction of 9*H*-fluoren-9-one and proceeds via 9,9′-bifluorenyl derivatives ($\triangleq$ Li_2[**7**]) such as 9-hydroxy-9,9′-bifluorenyl. The generally accepted mechanism rests on Wagner−Meerwein-type rearrangement of tetraphenylethylium ions such as [**D**]$^+$ (Scheme 5).[57] Given the

Scheme 5. Tetraphenylethylium Ion [D]$^+$ Is Thought To Link Dibenzo[*g*,*p*]chrysene and 9-Hydroxy-9,9′-bifluorenyl Under Clemmensen Conditions[a]

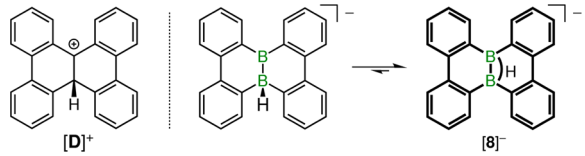

[a]The putative borane-borate carrying a terminal hydrogen substituent is the isoelectronic analogue of [D]$^+$. The anion was isolated in the form of its hydrogen-bridged isomer [**8**]$^-$; *t*Bu groups omitted.

isoelectronic relationship between carbenium ions and three-coordinate boranes, the tetraphenylethylium mechanism provides a plausible model to explain also the processes leading to Li_2[**6**]/Li_2[**7**] (see the SI for the detailed mechanistic proposal). In this scenario, borane-borates would act as analogues of tetraphenylethylium intermediates (e.g., [**8**]$^-$ is equivalent to [**D**]$^+$; Scheme 5). The required borane-borates might conceivably be generated through hydride exchange processes such as the ones taking place between K_2[**5**] and **4** (Scheme 4). However, if the borane-borate mechanism was indeed valid, K[**8**] would have to show a pronounced tendency to rearrange, but we always found it long-term stable in solution under inert conditions. We currently assume that the decisive difference between, e.g., [**D**]$^+$ and [**8**]$^-$ lies in the bridging hydrogen atom, which possibly shuts down 1,2-phenyl shifts in the boron species.

As an alternative to the borane-borate mechanism, the rearrangement cascade of **4** might be triggered by one-electron injection to create open-shell intermediates. Such a route would parallel the facile radical-promoted rearrangement of bifluorenylidene to dibenzo[*g*,*p*]chrysene. Harvey et al. have performed a detailed quantum-chemical study of the latter transformation[58] and the computed steps along the reaction coordinate are shown in Scheme 6 (left). An analogous

DOI: 10.1021/jacs.6b02303
J. Am. Chem. Soc. 2016, 138, 6224−6233

sequence can be written down also for the reduction of **4** (Scheme 6, right).

Scheme 6. Quantum-Chemically Calculated Mechanism of the Rearrangement Reaction Linking Dibenzo[*g*,*p*]chrysene and Bifluorenylidene (Left), and Analogous Reduction-Induced Sequence Explaining the Formation of $[5]^{2-}$, $[6]^{2-}$, and $[7]^{2-}$ from 4 (Right; Bold Indicates Isolated Species)[a]

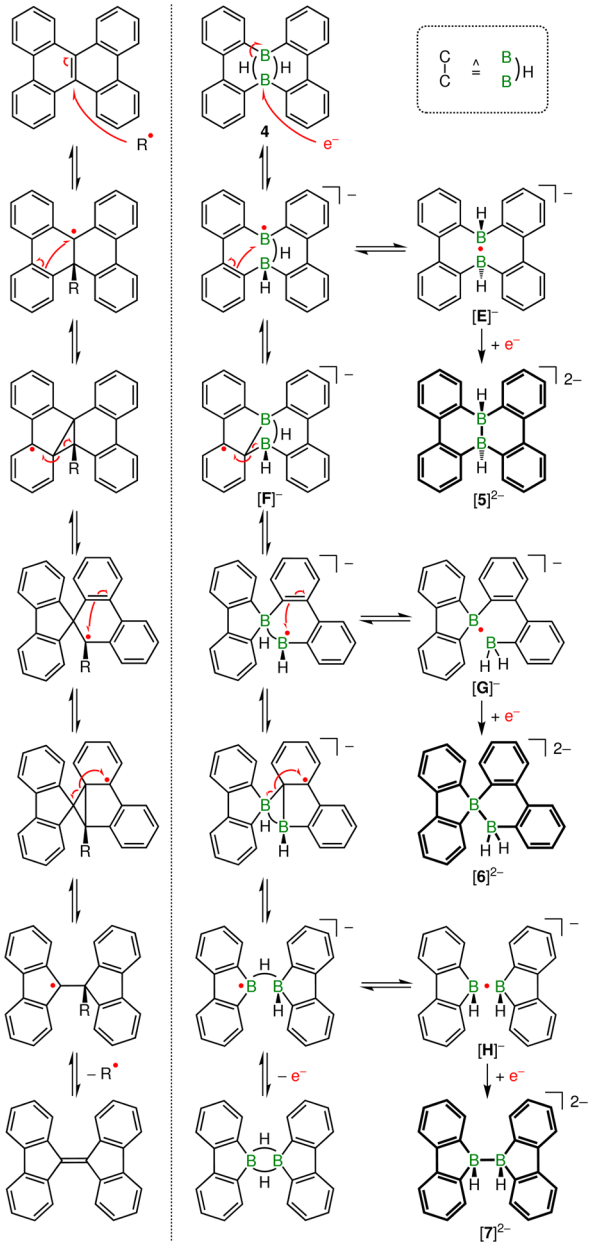

[a]In all boron compounds, *t*Bu groups were omitted for clarity.

Three general classes of reactions are involved: (i) electron injection, (ii) homolytic cleavage of a C=C π bond with concomitant formation of a B–C bond (and vice versa), (iii) hydrogen shift from a B–B bridging position to a terminal position accompanied by a shift of the odd electron into the space between the two B atoms.

The seemingly most exotic among the suggested boron intermediates are the B•B half-bonded (1e2c) species $[\mathbf{E}]^-$, $[\mathbf{G}]^-$, and $[\mathbf{H}]^-$. It is therefore important to recall the isolable and fully characterized B•B compounds Li[**I**] and Li[**J**],[39,41] which are structurally very similar to $[\mathbf{G}]^-$ and $[\mathbf{H}]^-$ (Figure 9a). Furthermore, $[\mathbf{H}]^-$ is a most plausible primary product of

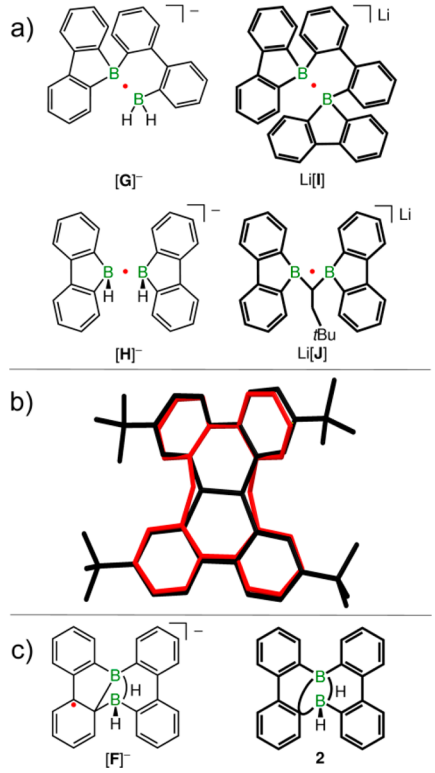

Figure 9. (a) Proposed B•B half-bonded reduction intermediates $[\mathbf{G}]^-$ and $[\mathbf{H}]^-$, and their synthetically accessible analogues Li[**I**] and Li[**J**]. (b) Overlay of the crystallographically determined molecular structure of $[\mathbf{5}]^{2-}$ (black) onto the calculated structure of its doubly oxidized congener **5′** (red; no B–B bond, no *t*Bu groups). (c) Proposed B–C–B-bridged radical intermediate $[\mathbf{F}]^-$ and the structurally related, isolable diborane(6) **2** (*t*Bu groups omitted).

the reduction of **3** and therefore provides an entry path for the experimentally observed reaction sequence ultimately leading to $[\mathbf{1}]^{2-}$ (cf. Scheme 1). With respect to $[\mathbf{E}]^-$, we note that the molecular backbones of its reduced form $[\mathbf{5}]^{2-}$ and its oxidized form **5′** (no B–B bond; calculated structure)[29] are virtually identical, apart from the larger B···B distance in **5′** (2.591 Å) as compared to $[\mathbf{5}]^{2-}$ (1.755(4) Å; cf. overlay of **5′** and $[\mathbf{5}]^{2-}$ in Figure 9b). Thus, a B•B 1e2c bond should likewise be compatible with the steric constraints imposed by the two 2,2′-biphenylene bridges. Finally, the molecular scaffold of $[\mathbf{F}]^-$ is reminiscent of the 9*H*-9-borafluorene dimer **2**, which we have used as starting material for the synthesis of **4** and $\mathrm{Li_2}[\mathbf{1}]$ (cf. Scheme 1 and Figure 9c).

The most important conclusion that can be drawn from the radical mechanism outlined in Scheme 6 relates to our initial question: *Why does the extent of skeletal rearrangement correlate with the amount of added reducing agent?*

The monoreduced radical anions are dynamic, but these processes come to an end as soon as the second reduction has taken place to give closed-shell products. If the reducing agent is in large supply (11 equiv of LiNaph/THF, 20 equiv of KC_8), a second electron becomes available immediately after the first electron has been accepted. The primary radical has not enough time to rearrange such that $\mathrm{Li_2}[\mathbf{1}]$ and $\mathrm{K_2}[\mathbf{5}]$ are obtained.

DOI: 10.1021/jacs.6b02303
J. Am. Chem. Soc. 2016, 138, 6224–6233

Lowering the amount of LiNaph or KC_8 to 4 equiv gives the radical time to rearrange at least once and to finally furnish $[\mathbf{6}]^{2-}$. In the presence of only 2 reduction equivalents, the radical can complete the full cascade and thereby form also $[\mathbf{7}]^{2-}$ after the second reduction step. Of course, up to a specific point in time an equilibrating mixture will not have generated one single species, but a distribution of several products in different stoichiometric ratios. Consequently, the reactions observed are not perfectly selective and this explains why we are usually facing more than one product.

CONCLUSION

Molecular chemistry is based upon the directed manipulation of covalent bonds. Underlying redistributions of the valence-electron shell can be investigated in their purest form by adding individual electrons without their accompanying atomic nuclei. In the systematic study presented herein, we have examined the reduction of 1,2:1,2-bis(4,4′-di-*tert*-butyl-2,2′-biphenylylene)-diborane(6) ($R_2B(\mu\text{-}H)_2BR_2$, **4**). Irrespective of the conditions applied, the formation of a B−B 2e2c bond could be achieved. In some cases, this process was accompanied by 1,2-phenyl shifts leading to the structurally characterized ring-contracted derivatives $Li_2[\mathbf{6}]$ and $Li_2[\mathbf{7}]$. The degree of rearrangement critically depends on the number of redox equivalents used and the way they are supplied. Excess reducing agent is helpful to suppress the rearrangement reactions. Under these conditions, KC_8 furnishes $K_2[R_2(H)B\text{−}B(H)R_2]$ ($K_2[\mathbf{5}]$) and Li granules or LiNaph/THF produce $Li_2[R_2B{=}BR_2]$ ($Li_2[\mathbf{1}]$), but no $Li_2[\mathbf{5}]$. A reason why $K_2[\mathbf{5}]$ is isolable whereas $Li_2[\mathbf{5}]$ remains elusive may be the higher heat of formation/lattice energy of LiH vs KH: Hydride abstraction from $[\mathbf{5}]^{2-}$ with concomitant double-electron injection would provide a straightforward route to $[\mathbf{1}]^{2-}$. Hydride transfer also plays a role in the reaction of **4** with 1 equiv of KC_8, which provides access to $K[(\mu\text{-}H)R_2B\text{−}BR_2]$ ($K[\mathbf{8}]$). In an independent experiment, a mixture of **4** and $K_2[\mathbf{5}]$ also gave $K[\mathbf{8}]$.

We finally outlined a closed-shell borane-borate as well as an open-shell mechanism, which could both account for the complex rearrangement scenario. Considering the currently available experimental data, we are inclined to prefer the radical mechanism. It not only explains how all experimentally observed products are generated, but also rationalizes the correlation between the product distribution and the amount of reducing agent employed.

ASSOCIATED CONTENT

Supporting Information

The Supporting Information is available free of charge on the ACS Publications website at DOI: 10.1021/jacs.6b02303.

Experimental details and characterization data (PDF)
X-ray crystallographic data (CIF)

AUTHOR INFORMATION

Corresponding Author

*matthias.wagner@chemie.uni-frankfurt.de

Notes

The authors declare no competing financial interest.

ACKNOWLEDGMENTS

T.K. and A.H. thank the Fonds der Chemischen Industrie for Ph.D. grants. Donations of lithium organyls by Rockwood Lithium GmbH are gratefully acknowledged.

REFERENCES

(1) Zhou, Z.; Wakamiya, A.; Kushida, T.; Yamaguchi, S. *J. Am. Chem. Soc.* **2012**, *134*, 4529−4532.
(2) Dou, C.; Saito, S.; Matsuo, K.; Hisaki, I.; Yamaguchi, S. *Angew. Chem., Int. Ed.* **2012**, *51*, 12206−12210.
(3) Saito, S.; Matsuo, K.; Yamaguchi, S. *J. Am. Chem. Soc.* **2012**, *134*, 9130−9133.
(4) Caruso, A., Jr.; Tovar, J. D. *Org. Lett.* **2011**, *13*, 3106−3109.
(5) Caruso, A., Jr.; Tovar, J. D. *J. Org. Chem.* **2011**, *76*, 2227−2239.
(6) Levine, D. R.; Caruso, A., Jr.; Siegler, M. A.; Tovar, J. D. *Chem. Commun.* **2012**, *48*, 6256−6258.
(7) Hoffend, C.; Schödel, F.; Bolte, M.; Lerner, H.-W.; Wagner, M. *Chem. - Eur. J.* **2012**, *18*, 15394−15405.
(8) Reus, C.; Weidlich, S.; Bolte, M.; Lerner, H.-W.; Wagner, M. *J. Am. Chem. Soc.* **2013**, *135*, 12892−12907.
(9) Berger, C. J.; He, G.; Merten, C.; McDonald, R.; Ferguson, M. J.; Rivard, E. *Inorg. Chem.* **2014**, *53*, 1475−1486.
(10) Hertz, V. M.; Bolte, M.; Lerner, H.-W.; Wagner, M. *Angew. Chem., Int. Ed.* **2015**, *54*, 8800−8804.
(11) Hertz, V. M.; Lerner, H.-W.; Wagner, M. *Org. Lett.* **2015**, *17*, 5240−5243.
(12) Schickedanz, K.; Trageser, T.; Bolte, M.; Lerner, H.-W.; Wagner, M. *Chem. Commun.* **2015**, *51*, 15808−15810.
(13) Miyamoto, F.; Nakatsuka, S.; Yamada, K.; Nakayama, K.; Hatakeyama, T. *Org. Lett.* **2015**, *17*, 6158−6161.
(14) For selected review articles on organoboron materials, see: (a) Entwistle, C. D.; Marder, T. B. *Angew. Chem., Int. Ed.* **2002**, *41*, 2927−2931. (b) Yamaguchi, S.; Wakamiya, A. *Pure Appl. Chem.* **2006**, *78*, 1413−1424. (c) Jäkle, F. *Chem. Rev.* **2010**, *110*, 3985−4022. (d) Hudson, Z. M.; Wang, S. *Dalton Trans.* **2011**, *40*, 7805−7816. (e) Rao, Y.-L.; Amarne, H.; Wang, S. *Coord. Chem. Rev.* **2012**, *256*, 759−770. (f) Lorbach, A.; Hübner, A.; Wagner, M. *Dalton Trans.* **2012**, *41*, 6048−6063. (g) Escande, A.; Ingleson, M. J. *Chem. Commun.* **2015**, *51*, 6257−6274.
(15) Doi, H.; Kinoshita, M.; Okumoto, K.; Shirota, Y. *Chem. Mater.* **2003**, *15*, 1080−1089.
(16) Wu, T.; Shen, H.; Sun, L.; Cheng, B.; Liu, B.; Shen, J. *New J. Chem.* **2012**, *36*, 1385−1391.
(17) Han, J.; Zhang, L. L.; Lee, S.; Oh, J.; Lee, K.-S.; Potts, J. R.; Ji, J.; Zhao, X.; Ruoff, R. S.; Park, S. *ACS Nano* **2013**, *7*, 19−26.
(18) Wu, Z.-S.; Ren, W.; Xu, L.; Li, F.; Cheng, H.-M. *ACS Nano* **2011**, *5*, 5463−5471.
(19) Fang, H.; Yu, C.; Ma, T.; Qiu, J. *Chem. Commun.* **2014**, *50*, 3328−3330.
(20) Lorbach, A.; Bolte, M.; Li, H.; Lerner, H.-W.; Holthausen, M. C.; Jäkle, F.; Wagner, M. *Angew. Chem., Int. Ed.* **2009**, *48*, 4584−4588.
(21) Januszewski, E.; Lorbach, A.; Grewal, R.; Bolte, M.; Bats, J. W.; Lerner, H.-W.; Wagner, M. *Chem. - Eur. J.* **2011**, *17*, 12696−12705.
(22) Seven, Ö.; Qu, Z.-W.; Zhu, H.; Bolte, M.; Lerner, H.-W.; Holthausen, M. C.; Wagner, M. *Chem. - Eur. J.* **2012**, *18*, 11284−11295.
(23) Hoffend, C.; Diefenbach, M.; Januszewski, E.; Bolte, M.; Lerner, H.-W.; Holthausen, M. C.; Wagner, M. *Dalton Trans.* **2013**, *42*, 13826−13837.
(24) Reus, C.; Guo, F.; John, A.; Winhold, M.; Lerner, H.-W.; Jäkle, F.; Wagner, M. *Macromolecules* **2014**, *47*, 3727−3735.
(25) Hübner, A.; Bolte, M.; Lerner, H.-W.; Wagner, M. *Angew. Chem., Int. Ed.* **2014**, *53*, 10408−10411.
(26) Bissinger, P.; Braunschweig, H.; Damme, A.; Kupfer, T.; Vargas, A. *Angew. Chem., Int. Ed.* **2012**, *51*, 9931−9934.
(27) Braunschweig, H.; Damme, A.; Dewhurst, R. D.; Vargas, A. *Nat. Chem.* **2013**, *5*, 115−121.
(28) Bissinger, P.; Steffen, A.; Vargas, A.; Dewhurst, R. D.; Damme, A.; Braunschweig, H. *Angew. Chem., Int. Ed.* **2015**, *54*, 4362−4366.
(29) Hübner, A.; Qu, Z.-W.; Englert, U.; Bolte, M.; Lerner, H.-W.; Holthausen, M. C.; Wagner, M. *J. Am. Chem. Soc.* **2011**, *133*, 4596−4609.

DOI: 10.1021/jacs.6b02303
J. Am. Chem. Soc. 2016, 138, 6224−6233

(30) Hübner, A.; Diefenbach, M.; Bolte, M.; Lerner, H.-W.; Holthausen, M. C.; Wagner, M. *Angew. Chem., Int. Ed.* **2012**, *51*, 12514−12518.
(31) For the corresponding Me_2S adduct, see: Das, A.; Hübner, A.; Weber, M.; Bolte, M.; Lerner, H.-W.; Wagner, M. *Chem. Commun.* **2011**, *47*, 11339−11341. For the NMR data of **3**, see the SI.
(32) Hübner, A.; Diehl, A. M.; Bolte, M.; Lerner, H.-W.; Wagner, M. *Organometallics* **2013**, *32*, 6827−6833.
(33) THF has only a negligible influence on the structural integrity of **4** under the conditions applied. According to ^{1}H NMR spectroscopy, a solution of the compound in THF-d_8 contains no **3** after 2 h at room temperature, about 1% after 4 d, and 5−10% after 30 d.
(34) Stock, A.; Laudenklos, H. *Z. Anorg. Allg. Chem.* **1936**, *228*, 178−192.
(35) (a) Klemm, L.; Klemm, W. *Z. Anorg. Allg. Chem.* **1935**, *225*, 258−261. (b) Hough, W. V.; Edwards, L. J.; McElroy, A. D. *J. Am. Chem. Soc.* **1956**, *78*, 689−689. (c) Hough, W. V.; Edwards, L. J.; McElroy, A. D. *J. Am. Chem. Soc.* **1958**, *80*, 1828−1829. (d) Hough, W. V.; Edwards, L. J. *Adv. Chem. Ser.* **1961**, *32*, 184−194. (e) Heřmánek, S.; Plešek, J. *Collect. Czech. Chem. Commun.* **1966**, *31*, 177−189. (f) Gaines, D. F.; Schaeffer, R.; Tebbe, F. *Inorg. Chem.* **1963**, *2*, 526−528.
(36) Godfroid, R. A.; Hill, T. G.; Onak, T. P.; Shore, S. G. *J. Am. Chem. Soc.* **1994**, *116*, 12107−12108.
(37) Shoji, Y.; Matsuo, T.; Hashizume, D.; Gutmann, M. J.; Fueno, H.; Tanaka, K.; Tamao, K. *J. Am. Chem. Soc.* **2011**, *133*, 11058−11061.
(38) Shoji, Y.; Kaneda, S.; Fueno, H.; Tanaka, K.; Tamao, K.; Hashizume, D.; Matsuo, T. *Chem. Lett.* **2014**, *43*, 1587−1589.
(39) Hübner, A.; Kaese, T.; Diefenbach, M.; Endeward, B.; Bolte, M.; Lerner, H.-W.; Holthausen, M. C.; Wagner, M. *J. Am. Chem. Soc.* **2015**, *137*, 3705−3714.
(40) In the meantime, also the dianion $[(NC)_3B{-}B(CN)_3]^{2-}$ has been synthesized: Landmann, J.; Sprenger, J. A. P.; Hailmann, M.; Bernhardt-Pitchougina, V.; Willner, H.; Ignat'ev, N.; Bernhardt, E.; Finze, M. *Angew. Chem., Int. Ed.* **2015**, *54*, 11259−11264.
(41) Hübner, A.; Diehl, A. M.; Diefenbach, M.; Endeward, B.; Bolte, M.; Lerner, H.-W.; Holthausen, M. C.; Wagner, M. *Angew. Chem., Int. Ed.* **2014**, *53*, 4832−4835.
(42) Braunschweig, H.; Dewhurst, R. D.; Mozo, S. *ChemCatChem* **2015**, *7*, 1630−1638.
(43) Evans, D. H.; Hu, K. *J. Chem. Soc., Faraday Trans.* **1996**, *92*, 3983−3990.
(44) The reduction potential of **4** is significantly more cathodic than the potentials of other arylboranes containing two tricoordinate boron atoms, cf. refs 7, 8, 10, 23.
(45) DuPont, T. J.; Mills, J. L. *J. Am. Chem. Soc.* **1975**, *97*, 6375−6382.
(46) Nakahama, S.; Hashimoto, K.; Yamazaki, N. *Polym. J.* **1973**, *4*, 437−445.
(47) Hatakeyama, T.; Hashimoto, S.; Seki, S.; Nakamura, M. *J. Am. Chem. Soc.* **2011**, *133*, 18614−18617.
(48) Eisch, J. J.; Kovacs, C. A.; Chobe, P. *J. Org. Chem.* **1989**, *54*, 1275−1284.
(49) Fox, M. A.; Whitesell, J. K. *Organic Chemistry*, 3rd ed.; Jones and Bartlett Publishers: Boston, Toronto, London, and Singapore, 2004.
(50) Grigsby, W. J.; Power, P. P. *J. Am. Chem. Soc.* **1996**, *118*, 7981−7988.
(51) Sridevi, V. S.; Leong, W. K.; Zhu, Y. *Organometallics* **2006**, *25*, 283−288.
(52) Littger, R.; Metzler, N.; Nöth, H.; Wagner, M. *Chem. Ber.* **1994**, *127*, 1901−1908.
(53) Wittig, G.; Barendt, E.; Schoch, W. *Justus Liebigs Ann. Chem.* **1971**, *749*, 24−37.
(54) Lammertsma, K.; Ohwada, T. *J. Am. Chem. Soc.* **1996**, *118*, 7247−7254.
(55) Holleman, A. F.; Wiberg, E.; Wiberg, N. *Lehrbuch der Anorganischen Chemie*, 101st ed.; de Gruyter: Berlin and New York, 1995.
(56) (a) Hertz, R. K.; Johnson, H. D., II; Shore, S. G. *Inorg. Chem.* **1973**, *12*, 1875−1877. (b) Khan, S. I.; Chiang, M. Y.; Bau, R.; Koetzle, T. F.; Shore, S. G.; Lawrence, S. H. *J. Chem. Soc., Dalton Trans.* **1986**, 1753−1757. (c) Wrackmeyer, B. *Z. Naturforsch., B: J. Chem. Sci.* **2004**, *59*, 1192−1199. (d) Pospiech, S.; Bolte, M.; Lerner, H.-W.; Wagner, M. *Chem. - Eur. J.* **2015**, *21*, 8229−8236.
(57) (a) Braunschweig, H.; Damme, A.; Dewhurst, R. D.; Kramer, T.; Kupfer, T.; Radacki, K.; Siedler, E.; Trumpp, A.; Wagner, K.; Werner, C. *J. Am. Chem. Soc.* **2013**, *135*, 8702−8707. (b) Harvey, R. G. *Polycyclic Aromatic Hydrocarbons*; Wiley-VCH: Weinheim and New York, 1997. (c) Talapatra, S. K.; Chakrabarti, S.; Mallik, A. K.; Talapatra, B. *Tetrahedron* **1990**, *46*, 6047−6052. (d) Suzuki, K. *Bull. Chem. Soc. Jpn.* **1962**, *35*, 735−740.
(58) Alder, R. W.; Harvey, J. N. *J. Am. Chem. Soc.* **2004**, *126*, 2490−2494.

DOI: 10.1021/jacs.6b02303
J. Am. Chem. Soc. 2016, 138, 6224−6233